

RESEARCH

Open Access



# Thrust measurements and mesothermal plasma plume of the Alternative Low Power Hybrid Ion Engine (*alphie*)

L. Conde<sup>1\*†</sup>, J. Gonzalez<sup>2†</sup>, J. M. Donoso<sup>1†</sup>, J. L. Domenech-Garret<sup>1†</sup> and M. A. Castillo<sup>3†</sup>

<sup>†</sup>L. Conde, J. Gonzalez, J.M. Donoso, J.L. Domenech-Garret and M.A. Castillo contributed equally to this work.

\*Correspondence: luis.conde@upm.es

<sup>1</sup> Departamento de Física Aplicada, Universidad Politécnica de Madrid, Cardenal Cisneros 3, 28040 Madrid, Spain

<sup>2</sup> DIFFER Dutch Institute for Fundamental Energy Research, De Zaale 20, Eindhoven 5612, AJ, The Netherlands

<sup>3</sup> Aernnova SAU, Avenida de Manoteras 20, 28050 Madrid, Spain

## Abstract

The high specific impulse Alternative Low Power Ion Engine (*alphie*) is a gridded plasma thruster different from conventional (Kaufman) ion engines. In this disruptive concept, the ionization of the propellant neutral gas and the neutralization of ion outflow is achieved with only one cathode located in front and outside of the thruster. Electrons and ions move under the self-consistent field created by the DC voltage applied to its two planar grids together with the currents of charges flowing through them, unlike to conventional ion engines, where only ions move through its ion optics system. The stationary mesothermal flow of ions and electrons in the plasma plume is characterized with a retarded field energy analyzer in conjunction with Langmuir and emissive probes. The ion velocity distribution functions and the electron energy spectra for different operating conditions of the *alphie* thruster are discussed. The observed high ion temperatures are explained by the collisional interaction between the fast ionizing electrons and the neutral atoms that increases their average kinetic energy. Finally, the *alphie* delivers 0.8–3.5 mN throttleable thrusts giving specific impulses in the range of 14000–20000 s with estimated thruster efficiencies between 8% and 40%.

**Keywords:** Ion engine, Plasma plume, Ion velocity distribution, Specific impulse

## Introduction

The high specific impulse of electric propulsion systems allows small satellites to perform multiple low-thrust maneuvers such as station-keeping, orbit-raising, and end-of-life disposal [1, 2]. Conventional chemical propulsion is generally not practical for these long-term operations due to payload limitations on these small spacecrafts. Multiple technologies have been tested in flight covering a wide range of electrical power consumption, however new disruptive approaches may enable better performance at lower cost and mass.

The new Alternative Low Power Ion Engine (*alphie*) is a promising new technology [3–6] for medium-sized satellites with electric power requirements below 500 W. This concept differs from classical ion engines (GIE) in two main features. First, it makes use of only one cathode disposed in front of the thruster for both ion neutralization and ionization propellant neutral gas. In second place, ions and electrons counterflow

through its two-grids system, unlike conventional GIE schemes, where only ions move through the grids.

In the *alphie*, electrons coming from the external cathode are accelerated inwards the ionization chamber by the same electrical potential drop that extracts and accelerates the ions outwards. These high energy electrons are magnetized in the ionization chamber where they collide with the propellant neutral gas, increasing its average kinetic energy and also are ionized. The ions are then extracted and accelerated outwards by the self-consistent electrical potential resulting from the ion and electron currents and the voltage applied to the grids [7]. Finally, additional electrons from the external cathode neutralize the outgoing ions to produce a quasineutral plasma plume. This basic operation scheme has been studied in the laboratory and also with particle-in-cell numerical simulations [3, 4, 7, 8]

As we shall see in the following sections, measurements of the ion velocity distribution functions in the plasma plume [4] show well collimated supersonic ion groups. Direct thrust measurements for propellant gas flows of  $Q = 0.2 - 0.6$  sccm of Argon give a throttleable thrusts between  $0.8 - 3.5$  mN, leading to specific impulses above 13.000 s.

This work is structured as follows, in Section 2 is introduced the *alphie* concept and operation, and the differences with conventional gridded ion thrusters. The distributions of ions and electrons in the plasma plume are discussed in Section 3 and the thrusts delivered in Section 4. Finally, conclusions are provided in Section 5.

### The *alphie* plasma thruster

Figure 1 is the cross-sectional schematic of the *alphie* plasma thruster (15 cm in length and 10 cm of diameter) with its electrical connections. Its specifics are discussed in detail in Refs. [3] and [4]. The local ground and the power supplies in Fig. 1 are electrically

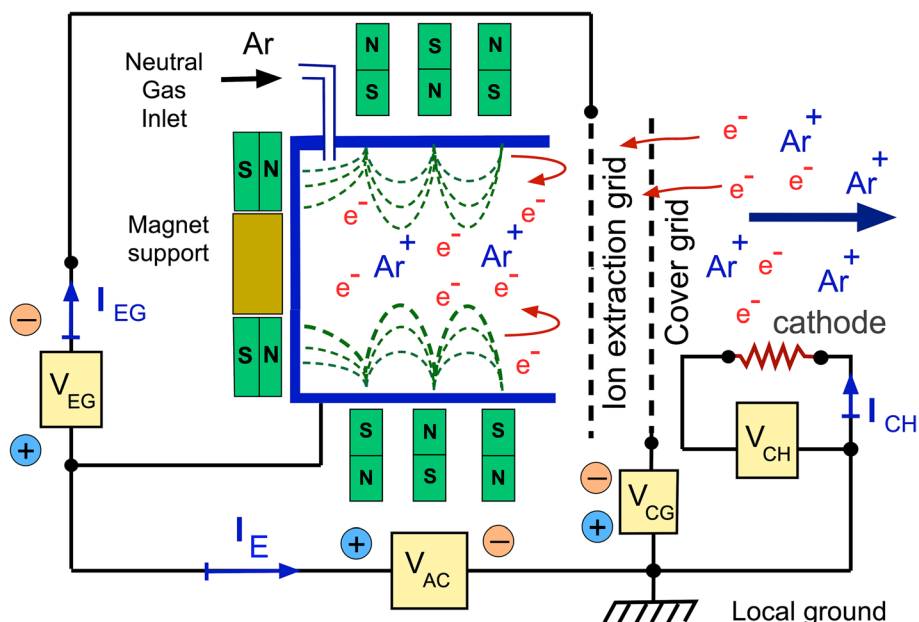


**Fig. 1** The cross-sectional schematic of the plasma thruster *alphie* with its electrical connections. The dashed lines indicate the magnetic field lines within the ionization chamber produced by the surrounding permanent magnets

insulated from the grounded walls of the vacuum tank. Thus, the *alphie* thruster is electrically floating with respect to its surroundings and the stream of charged particles is its only electrical connection with the diagnostic equipment and the vacuum tank.

The only cathode is located in front of the *cover* and ion *extraction* grids and it is negatively biased with respect to the ionization chamber by the voltage  $V_{AC}$ . Therefore, a fraction of emitted electrons move inwards the ionization chamber through the aligned holes of the grids. The *thruster current*  $I_E \gg I_{EG}$  characterizes the ion and electron currents flowing between the walls of the ionization chamber and the external cathode.

The acceleration voltage  $V_{AC}$ , within the 400 – 650 V range, is applied between the cover grid and the ionization chamber and the extraction potential  $V_{EG}$  is typically of 100 – 300 V. The control grid voltage  $V_{CG}$  in Fig. 1 is usually set to zero and can be used to stop electrons from entering the ionization chamber to interrupt the ion production process. The voltage  $V_{CG}$  is intended to cluster operation where two *alphie* thruster units share the acceleration voltage  $V_{AC}$  but have different control grid voltages. Hence, this configuration with two *alphie* units can provide a torque without turning off the power supplies that feed the thrusters.

The ionizing electrons moving inwards into the schematic of Fig. 1 are driven by the same potential drop  $V_{AC}$  as ions moving in the opposite direction. These incoming high-energy electrons are trapped by the magnetic field inside the ionization chamber and collide with the neutral gas atoms which may become ionized.

In addition to ionization, electron collisions transfer a large amount of energy to the neutral atoms within the ionization chamber of Fig. 1, increasing the average kinetic energy of gas atoms. This process results in the broad ion velocity distribution functions in the plasma plume that will be discussed below in Section 4. The ions are first extracted by the potential  $V_{EG}$  and later accelerated by the potential drop  $V_{AC}$  applied between the metallic walls of the ionization chamber and the cover grid. Finally, they leave the thruster and are neutralized by additional electrons coming from the external cathode.

The latter was made in this case by means of a thin tungsten wire heated to thermionic emission by the  $I_{CH}$  current as indicated in Fig. 1. This makes easier to study of the plasma plume, as it ensures that all of its ions have been produced by the *alphie* thruster, which is the only source of plasma in the experiments. However, other electron emitters such as conventional hollow cathodes or dispenser cathodes, can be also employed without affecting the thruster performance.

In the experiments discussed below, a flow of  $Q = 0.2 - 0.6$  sccm of Argon gas is introduced into the ionization chamber of Fig. 1, but the *alphie* thruster can also operate with Xenon or Krypton. For these Argon gas flows, the gas pressures in the vacuum tank were between  $1.0 \times 10^{-5}$  mbar and  $8.0 \times 10^{-5}$  mbar during the operation of the *alphie* thruster.

### Plasma plume structure

The physical properties of the stationary plasma plume of the *alphie* thruster along its  $Z$  axis of symmetry were determined using a combination of plasma diagnostics that can be displaced from the exit section of the thruster ( $z = 0$ ) along the  $(X, Y, Z)$  directions [9]. The ion velocity distribution functions (IVDF) were obtained using a four-grids retarded field energy analyzer (RFEA), which provides the one-dimensional ion

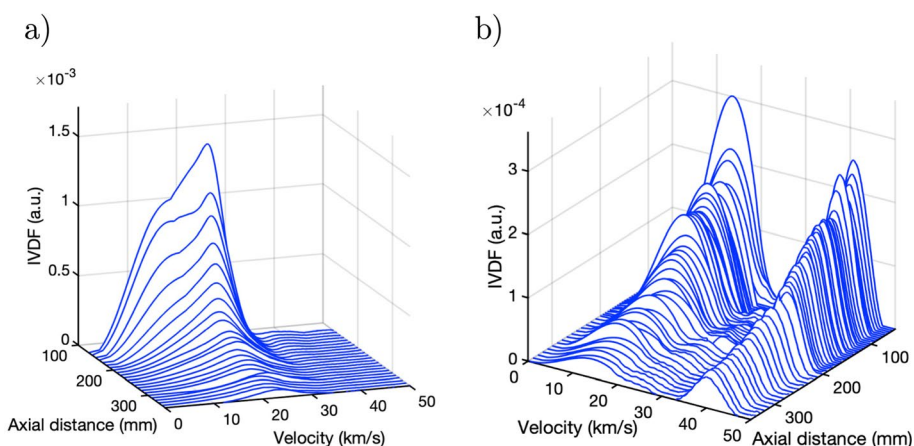
velocity spectra in arbitrary units. The electron energy distribution function (EEDF) were determined by a combination of Langmuir and emissive probes [10]. The details of the experimental setup and data analysis are in Refs. [4] and [9].

Figure 2 shows the waterfall representations of the IVDFs along symmetry axis of the plasma plume under two *alphie* thruster operating conditions. As Fig. 2a shows, for low acceleration voltages the distribution of ions with a single peak is observed within the velocity range of 10 – 30 km/s. When the acceleration voltage  $V_{AC}$  increases, two ion populations are clearly identified in Fig. 2b; A slow group with velocities of 10 – 20 km/s which for the fast ion population increases to the 35 – 45 km/s range.

Since for operating pressures the collisional mean free paths are much longer than the region studied in Fig. 2, the motion of ions in the plasma plume is collisionless. Therefore, the shape of the IVDFs remain essentially similar in Fig. 2b, and its value only decays due to the expansion of ions in the vacuum chamber. The ion temperatures for the fast  $T_{if} \simeq 60$  eV and slow  $T_{is} \simeq 35$  eV populations in Fig. 2 can be estimated from the IVDFs using the half width at half maximum approximation and remain essentially constant along the plasma plume.

The different geometrical expansion rates along the  $Z$  axis of symmetry of the fast and slow ion groups in Fig. 2b are evident in Fig. 3 when plotting the maxima of the IVDFs against the axial coordinate. Those in the high velocity group decay at a  $H(z) \sim z^{-1.5}$  rate while  $H(z) \sim z^{-2}$  for the slow population. Difference is due to the lower ratio  $v_z/v_r$  between axial  $v_z$  and radial  $v_r$  components of ion velocity in the latter. Consequently, the *alphie* thruster provides a population of ions with axial velocities of  $v_z \simeq 30 - 45$  km/s depending on the acceleration voltage [3].

Figures 4 and 5 show the velocities of the IVDFs maxima  $v_{mz}(x, y)$  for the slow and fast ion groups of Fig. 2b over a transversal cross section of the plasma plume. These velocities depend on the acceleration potential  $V_{AC}$  and are between 14 and 24 km/s for the slow ion population and in the range of 35 – 50 km/s for the fast ion group.



**Fig. 2** The waterfall representation of the IVDFs (in arbitrary units) along the  $Z$  axis of symmetry of the *alphie* plasma plume in two different operation conditions for the mass flow rate  $Q = 0.3$  sccm of Argon propellant gas. The ion group in **a** is for  $V_{AC} = 350$  V acceleration voltage and in **b** for  $V_{AC} = 500$  V two populations of ions develop

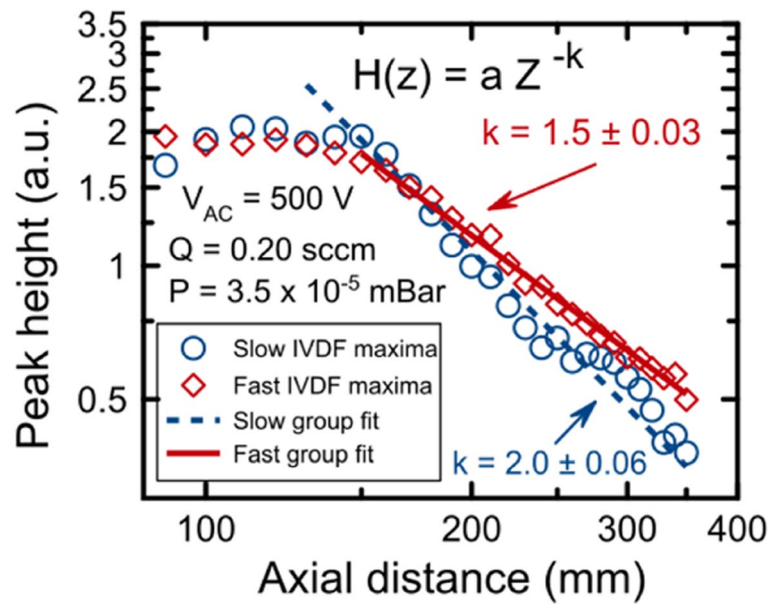


**Fig. 3** The velocities corresponding to the IVDF maxima of Fig. 2 represented against the axial coordinate  $Z$  on logarithm axes

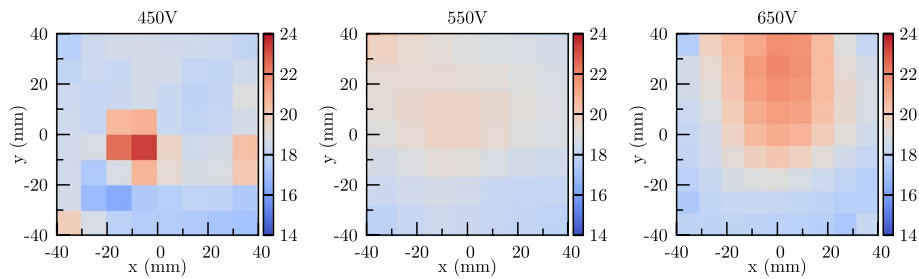


**Fig. 4** Velocities of IVDFs maxima  $v_{mz}(x, y)$  of the slow ion group over a transverse cross section  $(X, Y)$  of the plasma plume located at  $z = 150$  mm for  $V_{AC} = 450, 550$  and  $650$  V acceleration voltages. The color codes to the right of the figures are in km/s

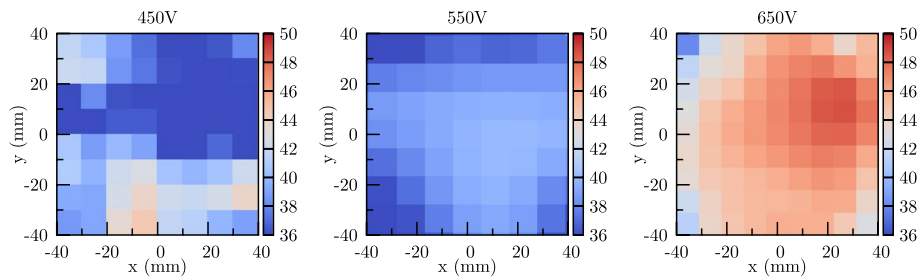


**Fig. 5** Velocities of IVDFs maxima  $v_{mz}(x, y)$  of the fast ion group over a transverse cross section  $(X, Y)$  of the plasma plume located at  $z = 150$  mm for  $V_{AC} = 450, 550$  and  $650$  V acceleration voltages. The color codes to the right of the figures are in km/s

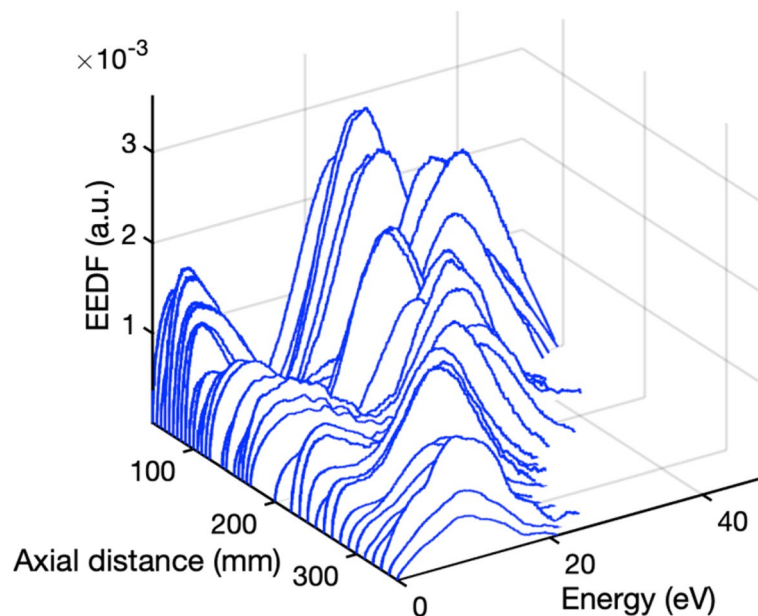
In both cases, the axial velocities of ions increase with the acceleration potential and for  $V_{AC} = 550$  V and become more evenly distributed along the cross section. Finally, for  $V_{AC} = 650$  V the ions concentrate in a narrower region and a collimated plasma beam develops of about 30 mm in diameter.

Figure 6 shows the electron energy distribution functions along the axis of symmetry  $Z$  of the plasma plume, obtained using the standard technique with the emissive and Langmuir probes [9, 10]. The dynamics of electrons is more complex than that of ions and EEDFs are the superposition of two distinct electron populations. The existence of multiple electron groups with different energies in the plasma plume expansion has been reported in previous studies with Helicon plasma sources [11, 12] and also in particle-in-cell numerical simulations [13].

The two groups of electrons observed close to the exit section of the *alphie* merge as the plasma plume expands. For typical distances  $z > 250$  mm away from the thruster only is observed a broad single peak in the EEDF. This electron energy thermalization process is not collisional, as the mean free paths for electron-neutral and electron-ion encounters are much longer than the region studied in Fig. 6.

The EEDFs of Fig. 6 allow estimating electron temperatures of  $T_e \sim 2.5 - 7$  eV along the plasma plume, which give ion sound velocities within the range of  $c_s \sim 6 - 11$  km/s. Consequently, most ions in Figs. 2, 4 and 5 have axial velocities faster than  $c_s$ . The *alphie* produces a *mesothermal* plasma flow where ion of mass  $M_i$  have velocities  $v_i \gg c_s$  but smaller the electron thermal speed  $v_{Te}$ ,

$$c^2 = \frac{k_B T_e}{M_i} \ll v_i^2 \ll \frac{k_B T_e}{m_e} = v_{Te}^2 \tag{1}$$



**Fig. 6** The waterfall representation of the EEDFs (in arbitrary units) along the axial coordinate of symmetry  $Z$  of the plasma plume

These *supersonic* ion velocities  $v_i$  are characteristic of plasma thrusters of high specific impulse  $I_{sp} = v_i/g_o$  where  $g_o$  is the standard Earth's acceleration [13].

### Efficiency and throttleable thrust

Figure 7 shows the measured impulses  $T$  by the *alphie* thruster as a function of the Argon gas mass flow rate  $Q$  and the acceleration voltage  $V_{AC}$ , since its throttle capability depends of these two parameters [4]. The delivered impulses are in the 0.8 – 3.5 mN range and the specifics of the thrust measurement system employed are discussed in Ref. [14].

The control of thrust using the acceleration potential  $V_{AC}$  in Fig. 7a, is in agreement with the increment in the velocities of IVDFs maxima of the slow and fast ion groups observed in Figs. 4 and 5. As Fig. 7b shows, the impulse delivered also can be regulated using the propellant gas mass flow rate.

In Fig. 7a the impulse increases linearly with  $Q$  for  $V_{AC} = 650$  V and the growing rates are lower for smaller acceleration voltages. This effect is related to the specifics of the *alphie* operation in which electrons from the external cathode ionize the propellant neutral gas. Thruster performance is affected by the increased gas mass flow rates combined with a reduced ionizing electron flow at lower  $V_{AC}$  voltages.

The specific impulses  $I_{sp} = T/(\dot{m}g_o)$  calculated from the delivered thrusts in Fig. 7 are of 14000 – 20000 s for Argon gas and are higher than the ratio  $I_{sp} = v_i/g_o \simeq 4400$  s obtained with the peak drift speed of the fast ion group in Fig. 2. This discrepancy can be explained by the additional contributions to the thrust of the slow ion group, together with the elevated exhaust velocity of neutrals. The latter results from the collisional gas heating inside the ionization chamber of Fig. 1 by ionizing electrons from the cathode. Their motion inside is essentially limited along the magnetic field lines produced by a set of permanent magnets as shows Fig. 1.

For energies over 100 eV, the collisional cross sections for ionization, momentum transfer and elastic cross sections for Argon of  $(0.7 - 2.0) \times 10^{-15}$  cm<sup>2</sup> are similar. The average velocity of neutrals is increased by the collisional transference of energy by fast electrons from the cathode and, simultaneously the propellant gas becomes partially ionized.

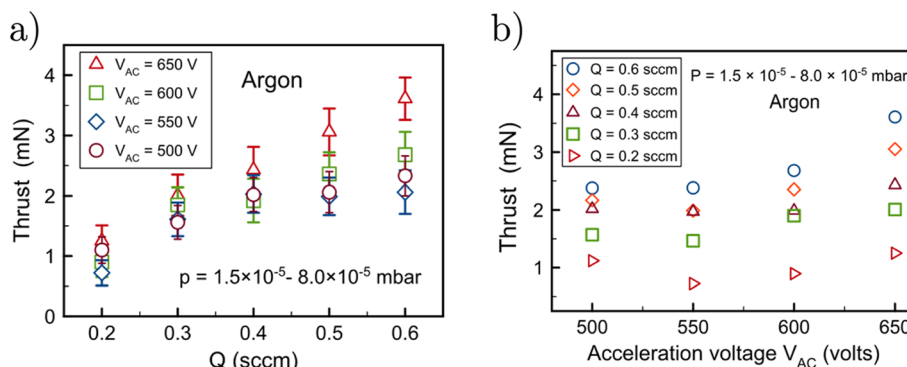


**Fig. 7** The impulses delivered by the *alphie* thruster represented in **a** against the Argon propellant mass flow rate and in **b** as a function of the acceleration potential. The error are of  $\pm 0.4$  mN in all cases and are not depicted in Fig. **b** for clarity

Therefore, ions in Fig. 2 have a similar energy distribution around the average velocity than neutral gas atoms before the ionizing collision [4]. The high temperatures of the ions  $T_{if} \simeq 60$  eV and  $T_{is} \simeq 60$  eV for the slow and fast ion groups are explained by the transfer of energy from fast electrons coming from the external cathode to the atoms of propellant neutral gas [4].

The electric power intake of the *alphie* thruster is typically within the  $W = 200 - 350$  W range at low and high acceleration voltages. The kinetic power can be estimated as  $P_W = T \times v_{mi}$  where  $v_{mi}$  is an average velocity of the exhausted particles, that can be approximated by the velocities  $v_i \sim 20 - 40$  km/s corresponding to the maxima of the IVDFs. These give thruster efficiencies of  $\eta = P_W/W \sim 8\% - 40\%$  using the range of thrusts in Fig. 7.

## Conclusions

The recently introduced *alphie* thruster in [3–6], is a disruptive concept of a gridded engine when compared to conventional (Kaufman) gridded ion engines in which only ions are transported through the ion optics system [1]. In the *alphie* scheme, both positive and negative charges move through the open spaces of its two-grids system along opposite directions under the same self-consistent electric field. The latter is produced by the DC electric potential applied to the grids and the currents of exiting ions and ionizing electrons moving inwards. This basic operation principle has been studied in the laboratory and also with numerical simulations [3, 4, 7, 8].

Figure 2 shows that the *alphie* thruster expels an ion stream that splits into fast and slow supersonic ion groups at high  $V_{AC}$  acceleration potentials. The slow ion group originates from resonant and non-resonant charge exchange collisions with neutral gas atoms leaking through the aligned holes of the two grids.

The velocity of ions in the IVDFs of Fig. 2 results from two different physical mechanisms. In first place, the collisional increase in the temperature of the neutral gas inside the ionization chamber, next the subsequent acceleration of the ions along the axial direction by the self-consistent electric field established in the open spaces of the grids.

This two-stage process delivers the throttleable impulses of Fig. 7, which can be controlled by either, the acceleration potential  $V_{AC}$  and the propellant mass flow rate  $Q$ . The high specific impulses  $I_{sp} = T/(\dot{m} g_0)$  of the *alphie* thruster are not only due to the average speed of the fast group of IVDFs in Fig. 2 since the slow ion population and the high average velocity of neutrals resulting from collisional electron heating also contribute to the thrust delivered.

The complex dynamics of electrons in the axial direction of the plasma plume shown in Fig. 6 requires further study. Due to its lower mass and high speeds, there may be contributions from radial electron flows produced by small changes in the plasma potential.

The characterization of the *alphie* thruster performance for Xenon and Krypton will be carried out soon as well as the detailed study of the ion velocity distributions along the transverse directions to the axis of symmetry of the plasma plume.

## Acknowledgements

The authors are grateful for the technical assistance of Mr. F. Sánchez. The authors acknowledge the funding by the Spanish Government through grant RT2018-094409-B-100 by the *Agencia Estatal de Investigación* of Spain and also by the European Union, *ERDF A way of making Europe*.

**Authors' contributions**

LC and JG managed the conceptualization, methodology and writing of the manuscript; JMD, JLDG and MAC were in charge of data collection and analysis. All authors read and approved the final manuscript.

**Funding**

The research leading to these results received funding from the *Agencia Estatal de Investigación of Spain under grant RT2018-094409-B-100*.

**Availability of data and materials**

The data that support the findings of this study are available from the corresponding author upon reasonable request.

**Declarations****Ethics approval and consent to participate**

Not applicable.

**Consent for publication**

The authors give their consent for publication.

**Competing interests**

The authors declare that they have no competing interests.

Received: 24 August 2022 Accepted: 31 October 2022

Published online: 14 November 2022

**References**

1. Goebel D, Katz I (2008) Fundamentals of electric propulsion: Ion and Hall thrusters. Wiley, Hoboken. <https://doi.org/10.1002/9780470436448>
2. Mazouffre S (2016) Electric propulsion for satellites and spacecraft: established technologies and novel approaches. *Plasma Sour Sci Technol* 25(3):033002. <https://doi.org/10.1088/0963-0252/25/3/033002>
3. Conde L, Domenech-Garret J, Donoso J, Damba J, Tierno S, Alamillo-Gamboa E, Castillo M (2017) Supersonic plasma beams with controlled speed generated by the alternative low power hybrid ion engine (alphie) for space propulsion. *Phys Plasmas* 24(12):123514. <https://doi.org/10.1063/1.5005881>
4. Conde L, Maldonado P, Damba J, Gonzalez J, Domenech-Garret J, Donoso J, Castillo M (2022) Physics of the high specific impulse alternative low power hybrid ion engine (alphie): Direct thrust measurements and plasma plume kinetics. *J Appl Phys* 131(2):023302. <https://doi.org/10.1063/5.0067214>
5. Conde L, Domenech-Garret JL, Donoso JM, Del Río E, Castillo MA (2019) Plasma accelerator with modulated thrust. US Patent No. 10,172,227 B2
6. Conde L, Domenech-Garret JL, Donoso JM, Del Río E, Castillo MA (2015) Plasma accelerator with modulated thrust and space born vehicle with the same. European Patent EP3369294B1
7. González J, Conde L (2019) Particle-in-cell simulations of the extraction and acceleration processes in the alternative low power hybrid ion engine (alphie). *Phys Plasmas* 26(4):043505. <https://doi.org/10.1063/1.5084242>
8. Dyubo D, González J, Tsybin O, Conde L (2021) Charge transport characterization of the alternative low power hybrid ion engine (alphie) with particle-in-cell simulations. *Phys Plasmas* 28(10):103509. <https://doi.org/10.1063/5.0060260>
9. Damba J, Argente P, Maldonado P, Cervone A, Domenech-Garret J, Conde L (2018) Multiprobe characterization of plasma flows for space propulsion. *J Phys Conf Ser* 958(012002–1):9. <https://doi.org/10.1088/1742-6596/958/1/012002>
10. Hershkovitz N (1989) How langmuir probes work. In: Auciello O, Flamm D (eds) *Plasma Diagnostics Discharge Parameters and Chemistry*, chap 4. Academic Press, London, pp 113–183
11. Aguirre E, Scime E, Thomson D, Good T (2017) Spatial structure of ion beams in an expanding plasma. *Phys Plasmas* 24(123510–1):11. <https://doi.org/10.1063/1.5003722>
12. Aguirre E, Bodin R, Yin N, Scime E (2020) Evidence of electron energization accompanying spontaneous formation of ion acceleration regions in expanding plasmas. *Phys Plasmas* 27(123501–1):8. <https://doi.org/10.1063/5.0025523>
13. Hu Y, Wang J (2015) Electron properties in collisionless mesothermal plasma expansion: Fully kinetic simulations. *IEEE Trans on Plasma Sci* 43(9):2832–2838. <https://doi.org/10.1109/TPS.2015.2433928>
14. Conde L, Lahoz M, Grabulosa J, Hernández R, González J, Delgado M, Damba J Thrust stand based on a single point load cell for impulse measurements from plasma thrusters. *Rev Sci Instrum* 81(2):023308–1,6. <https://doi.org/10.1063/1.5127189>

**Publisher's Note**

Springer Nature remains neutral with regard to jurisdictional claims in published maps and institutional affiliations.